Taylor & Francis
Taylor & Francis Group

Journal of Toxicology and Environmental Health, Part A

ISSN: 1528-7394 (Print) 1087-2620 (Online) Journal homepage: https://www.tandfonline.com/loi/uteh20

Role of Inducible Nitric Oxide Synthase-Derived Nitric Oxide in Silica-Induced Pulmonary Inflammation and Fibrosis

Patti C. Zeidler , Ann Hubbs , Lori Battelli & Vincent Castranova

To cite this article: Patti C. Zeidler , Ann Hubbs , Lori Battelli & Vincent Castranova (2004) Role of Inducible Nitric Oxide Synthase-Derived Nitric Oxide in Silica-Induced Pulmonary Inflammation and Fibrosis, Journal of Toxicology and Environmental Health, Part A, 67:13, 1001-1026, DOI: 10.1080/15287390490447296

To link to this article: https://doi.org/10.1080/15287390490447296

Journal of Toxicology and Environmental Health, Part A, 67:1001–1026, 2004

ISSN: 1528–7394 print / 1087–2620 online
DOI: 10.1080/15287390490447296

ROLE OF INDUCIBLE NITRIC OXIDE SYNTHASE-DERIVED NITRIC OXIDE IN SILICA-INDUCED PULMONARY INFLAMMATION AND FIBROSIS

Patti C. Zeidler,[1] Ann Hubbs,[2] Lori Battelli,[2] Vincent Castranova[1]

[1]National Institute for Occupational Safety and Health, Health Effects Laboratory Division, and Department of Physiology and Pharmacology, West Virginia University, Morgantown, West Virginia, USA
[2]National Institute for Occupational Safety and Health, Health Effects Laboratory, Morgantown, West Virginia, USA

Inhalation of crystalline silica can produce lung inflammation and fibrosis. Inducible nitric oxide synthase (iNOS)-derived nitric oxide (NO) is believed to be involved in silica-induced lung disease. To investigate the role of iNOS-derived NO in this disease, the responses of iNOS knockout (KO) versus C57Bl/6J wild-type (WT) mice to silica were compared. Male mice (8–10 wk old, mean body weight 24.0 g) were anesthetized and exposed, by aspiration, to silica (40 mg/kg) or saline. At 24 h and 42 d postexposure, lungs were lavaged with saline. The first bronchoalveolar lavage (BAL) fluid supernatant was analyzed for lactate dehydrogenase (LDH) activity, levels of albumin, tumor necrosis factor-α (TNF-α), and macrophage inflammatory protein-2 (MIP-2), as well as total antioxidant capacity (TAC). The cellular fraction of the total BAL was used to determine alveolar macrophage (AM) and polymorphonuclear leukocyte (PMN) counts, and zymosan-stimulated AM chemiluminescence (AM-CL). In separate mice, lung histopathological changes were evaluated 42 d postexposure. Acute (24-h) silica exposure decreased AMs, increased PMNs, increased LDH activity and levels of albumin, TNF-α, and MIP-2 in BAL fluid, and enhanced AM-CL in both iNOS KO and WT mice. However, iNOS KO mice exhibited less AM activation (defined as increased AM-CL and decreased AM yield) than WT. Furthermore, TAC following acute silica decreased in WT but was maintained in iNOS KO mice. Pulmonary reactions to subchronic (42 d) silica exposure were similar to acute. However, histopathological and BAL fluid indices of lung damage and inflammation, AM activation, and lung hydroxyproline levels were significantly less in iNOS KO compared to WT mice. These results suggest that iNOS-derived NO contributes to the pathogenesis of silica-induced lung disease in this mouse model.

Inhalation of crystalline silica in various occupational settings, including sandblasting, quarrying, stone dressing, refractory manufacture, or foundry work, can result in silicosis (Mossman & Churg, 1998). Various clinical and pathological forms of the disease exist including acute, accelerated, and chronic silicosis,

Received 23 October 2003; accepted 15 December 2003.
The authors hereby state that no conflicts of interest exist with this article.
Address correspondence to Vincent Castranova, Pathology and Physiology Research Branch, Health Effects Laboratory Division, National Institute for Occupational Safety and Health, 1095 Willowdale Road, M/S 2015, Morgantown, WV 26505, USA. E-mail: vic1@cdc.gov

which depend on the level of dust exposure and the resulting latency period for disease initiation and progression.

Silica occurs naturally either in noncrystalline (amorphous) or crystalline forms. Crystalline silica, as compared to amorphous varieties, is known to be more pathogenic in humans and is composed of silicon and oxygen (SiO_2) with trace quantities of Al, Fe, Mn, Mg, Ca, and Na (Mossman & Churg, 1998). α-Quartz, used in the present study, is the most common form of crystalline silica. This particular form comprises nearly 67% of granite, shale, and sandstone; thus, significant exposure can occur in occupations that involve blasting, grinding, or fracturing of these rocks (Mossman & Churg, 1998).

Reactive species produced either by silica or silica-stimulated cells are proposed to be mediators of silica-induced inflammation, cytotoxicity, DNA modifications, and fibrosis (Shukla et al., 2001; Vallyathan et al., 1998; Daniel et al., 1993; Shi et al., 1998). Nitric oxide (NO) is a reactive nitrogen species recently implicated in the pathogenesis of silica-induced lung disease (Porter et al., 2002; Srivastava et al., 2002). NO is formed from the conversion of the amino acid L-arginine to L-citrulline in the presence of various cofactors and the enzyme nitric oxide synthase (NOS) (Rao, 2000). There are three described isoforms of NOS, inducible NOS (iNOS or NOS2), and the constitutive NOS isoforms endothelial (eNOS or NOS3) and neuronal (nNOS or NOS1). iNOS is produced in various lung cells in response to inflammatory stimuli, such as endotoxin (Mikawa et al., 1998).

The role of iNOS-derived NO in particle-induced lung disease remains unclear with both anti-inflammatory and proinflammatory mechanisms being described (Zeidler & Castranova, 2004). Conflicting data show NO may inhibit or enhance the activation of nuclear factor-κB (NF-κB), which ultimately affects the production of inflammatory cytokines (Chen et al., 1995; Kang et al., 2000). NO also increases lung inflammation and damage by combining with superoxide ($O_2^{\cdot}$) to form peroxynitrite ($OONO^-$), a highly reactive species that produces lipid peroxidation, mitochondrial and DNA damage, and enzyme and protein inactivation (Hogg & Kalyanaraman, 1999; van der Vliet et al., 1997; Haddad et al., 1996a, 1996b).

Intratracheal instillation and inhalation exposures in rats show increased NO production is associated with the lung injury produced by silica. Blackford et al. (1997) reported that iNOS mRNA induction in bronchoalveolar lavage (BAL) cells and NO-dependent chemiluminescence from alveolar macrophages (AMs) correlated with the degree of pulmonary inflammation produced by intratracheal instillation of rats with silica, coal, carbonyl iron, or titanium dioxide. Furthermore, a chronic rat silica inhalation study by Porter et al. (2002) showed a temporal correlation between lung NO production and pulmonary inflammation and fibrosis. Immunohistochemistry data also revealed that silicotic lesions in the lung were associated with iNOS staining and nitrotyrosine residues. In humans, Castranova et al. (1998) reported that AMs harvested from coalminers exposed chronically to silica-containing dusts displayed enhanced NO-dependent chemiluminescence and iNOS mRNA induction compared to AMs from a healthy

nonsmoking subject, with NO induction associated with disease progression determined by chest radiographs.

The evidence presented thus far reported associations between iNOS-derived NO and silica-induced lung disease. However, a causal link has yet to be determined. A model of iNOS-derived NO deficiency, the iNOS knockout (iNOS KO), mouse, has recently been employed in studies involving endotoxin, asbestos, and silica to further examine the role of this inflammatory mediator. Intratracheal instillation of asbestos in iNOS KO mice, for example, resulted in an enhanced pulmonary inflammatory response [higher tumor necrosis factor-α (TNF-α) production and neutrophil influx] but attenuated oxidant-promoted lung tissue damage as measured by decreased protein leakage and lactate dehydrogenase (LDH) release into the alveolar space (Dorger et al., 2002). In addition, attenuation of silica-induced lung disease in iNOS KO mice was reported in a histological study by Srivastava et al. (2002). The present study will further investigate iNOS-derived NO in a model of silica-induced pulmonary damage, inflammation, and fibrosis by comparing the acute (24 h) and subchronic (42 d) pulmonary responses in wild-type (WT) versus iNOS KO mice.

METHODS

Animals

Breeder pairs of iNOS knockout (B6.129P2-Nos2^{tm1Lau}) mice along with wild-type strain mice (C57Bl/6J) were purchased from Jackson Laboratories (Bar Harbor, ME). Offspring of iNOS knockout mice and wild type mice were age and weight matched for this study, that is, 8–10 wk old with a mean body weight of 24.0 g (23.4 g for KO mice and 24.8 g for WT mice). Animals were housed in an AAALAC-accredited, specific-pathogen-free, environmentally controlled facility and allowed to acclimate at least 5 d prior to use. The mice were free of endogenous viral pathogens, parasites, mycoplasms, *Helicobacter*, and CAR *Bacillus*. Mice were kept in ventilated cages, which were provided HEPA-filtered air, with Alpha-Dri virgin cellulose chips and hardwood Beta-chips for bedding. Food and tap water were given ad libitum. All animal procedures were performed in accordance with an approved ACUC protocol (number 02-VC-M-018).

Mouse Pharyngeal Aspiration

Mouse pharyngeal aspiration was performed as described by Rao et al. (2003), except the present study anesthetized the mice using a mixture of ketamine and xylazine (50 and 2 mg/kg subcutaneous in the abdominal area, respectively). Following anesthesia, the animals were placed on a board in a near vertical position and the animal's tongue extended with lined forceps. A suspension (~30 μl) of heat-sterilized aged Min-U-Sil 5 silica (98.5% crystalline silica, particle diameter <5 μm, U.S. Silica, Berkeley Springs, WV) at a dose of

40 mg/kg was placed posterior in the throat and the tongue held until the suspension was aspirated into the lungs. Control mice were administered sterile $Ca^{2+}+Mg^{2+}$-free phosphate-buffered saline (PBS) vehicle (pH 7.4). The mice revived unassisted after approximately 30–40 min. All mice survived this procedure. Rao et al. (2003) have shown that the pharyngeal aspiration technique results in a uniform deposition of particles within the mouse lung. Mice were sacrificed either 24 h or 42 d following aspiration. These postexposure times were chosen to evaluate the role of iNOS-derived NO in both the acute and subchronic response to silica exposure.

Bronchoalveolar Lavage

Mice were weighed (mean body weight 24.0 g) and euthanized with an intraperitoneal injection of sodium pentobarbital (>100 mg/kg). The trachea was cannulated with a blunted 22-gauge needle and bronchoalveolar lavage (BAL) was performed using cold sterile $Ca^{2+}+Mg^{2+}$-free PBS at a volume of 0.6 ml for first lavage (kept separate) and 1 ml for subsequent lavages. Approximately 10 ml BAL fluid per mouse was pooled and collected in sterile centrifuge tubes. Typically, BAL fluid from two to three mice was pooled to obtain a sufficient cell number to conduct assays for a single experiment. Pooled BAL cells were washed in PBS by alternate centrifugation ($600\times g$ for 10 min at 4 °C) and resuspension. Acellular first-fraction BAL aliquots were frozen or kept on ice for later analysis. The final cell pellet was suspended in 10 m*M* HEPES buffer (145 m*M* NaCl, 5 m*M* KCl, 10 m*M* HEPES, 1 m*M* $CaCl_2$, 5.5 m*M* glucose) at pH 7.4.

Cell Counts and Differentials

Cell counts were performed using an electronic cell counter equipped with a cell sizing attachment (Coulter model Multisizer II with a 256C channelizer, Coulter Electronics, Hialeah, FL). Alveolar macrophages or polymorphonuclear leukocytes were identified by their characteristic cell diameter (Castranova et al., 1990).

First Bronchoalveolar Lavage Tumor Necrosis Factor-α, Macrophage Inflammatory Protein-2, and Transforming Growth Factor-β1 Assays

First BAL fluid was assayed using a mouse TNF-α, a multispecies transforming growth factor-β1 (TGF-β1) (BioSource International, Camarillo, CA), or a mouse macrophage inflammatory protein-2 (MIP-2) enzyme-linked immunosorbent assay (ELISA) kit (R & D Systems, Minneapolis, MN) according to manufacturers' instructions. First BAL fluid was diluted 1.9-fold in the TGF-β1 assay and the TNF-α and MIP-2 assays required undiluted first BAL fluid. Concentrations of TNF-α, TGF-β1, and MIP-2 were determined as picograms per milliliter based on the appropriate standard curve. ELISA plates were read at 450 nm using a Spectramax 250 microplate spectrophotometer (Molecular Devices Corporation, Sunnyvale, CA).

Primary Mouse Alveolar Macrophage Zymosan-Stimulated Chemiluminescence

Alveolar macrophage (AM) chemiluminescence was determined as described by Porter et al. (2002) using an automated luminometer (Berthold Autolumat LB 953, EG & G, Gaithersburg, MD) at 390–620 nm for 15 min with a total assay volume of 0.25 ml. Briefly, 1×10^6 alveolar macrophages/ml from control or silica-exposed mice were incubated in HEPES buffer, and resting chemiluminescence was determined by adding 5-amino-2,3-dihydro-1,4-phthalazinedione (luminol) at a final concentration of 0.08 μg/ml. Zymosan-stimulated chemiluminescence was determined by adding unopsonized zymosan A (Sigma, St. Louis, MO) at 2 mg/ml immediately before measurement. Unopsonized zymosan has been shown to stimulate chemiluminescence from alveolar macrophages but not polymorphonuclear leukocytes, which only respond to opsonized particles (Castranova et al., 1987a; Hill et al., 1977; Allen, 1977). Zymosan-stimulated chemiluminescence was calculated as counts per minute (cpm) in the zymosan-stimulated assay minus cpm in the resting assay.

First Bronchoalveolar Lavage Fluid Albumin

Albumin concentration (mg/ml) was determined colorimetrically at 628 nm based on albumin binding to bromcresol green (Albumin BCG diagnostic kit, Sigma, St. Louis, MO) using a Cobas Mira Plus transfer analyzer (Roche Diagnostic Systems, Montclair, NJ).

First Bronchoalveolar Lavage Fluid Lactate Dehydrogenase

Lactate dehydrogenase (LDH, U/L) activity was determined by monitoring the LDH-catalyzed oxidation of pyruvate coupled with the reduction of NAD at 340 nm using a commercial kit and a Cobas Mira Plus transfer analyzer (Roche Diagnostics Systems, Montclair, NJ).

First Bronchoalveolar Lavage Fluid Total Antioxidant Capacity

Total antioxidant capacity was assessed using the Bioxytech AOP-490 assay (Oxis Research, Portland, OR), which is based on the reduction of Cu^{2+} to Cu^{+} by all antioxidants in the sample. Using a SpectraMax 250 microplate spectrophotometer (Molecular Devices Corporation, Sunnyvale, CA) set to 490 nm, data were obtained from a standard curve of known uric acid concentrations and expressed as "mM Uric Acid Equivalents."

Determination of NOx: Nitrate (NO_3^-) and Nitrite (NO_2^-)

AMs (2×10^5 cells/well) from WT mice exposed to silica or saline in vivo for 42 d were plated in a 24-well tissue culture plate and allowed to adhere for 90 min at 37 °C. The wells were washed three times to remove nonadherent cells. Cells were incubated for an additional 18 h and after centrifugation the acellular supernatants were harvested and NOx was determined by flow injection

analysis colorimetry at 540 nm, using the Griess reaction (Quick-Chem 8000, Lachat Instruments, Milwaukee, WI) as described by Porter et al. (2002).

Lung Hydroxyproline

Mice were euthanized using sodium pentobarbital ip (>100 mg/kg) at 42 d postexposure. Lungs were removed en bloc, weighed, and snap frozen in liquid nitrogen then frozen at −80 °C for later analysis. Lung tissue was processed to determine hydroxyproline content, according to previously described methods (Kivirikko et al., 1967; Ma et al., 1999). Briefly, lungs were finely minced and placed in individual capped glass test tubes with 1 ml of 6 *N* HCl. Lungs were acid digested for 2 d at 110 °C. Samples were centrifuged (500 × *g*) for 1 h, and the hydrolysate was neutralized to pH 7 using KOH and brought to a final volume of 3.7 ml in deionized H_2O. In capped glass test tubes, 0.3 ml hydrolysate was added to 2.2 ml borate-alanine buffer (2:1 ratio of potassium borate buffer [12.37 g boric acid and 45 g KCl in 200 ml deionized H_2O, pH 8.7] and alanine solution [10 g alanine in 100 ml deionized H_2O), pH 8.7]). Saturating amounts of solid KCl were added to samples and hydroxyproline standards (standard range 0–28 μg) followed by 0.6 ml of 0.2 *M* chloramine T (2.254 g in 40 ml ethylene glycol monomethyl ether). After oxidation at room temperature for 40 min, 2 ml of 3.6 *M* $Na_2S_2O_3$ was used to stop oxidation. After addition of 2.5 ml toluene, samples were placed in a boiling water bath for 30 min, then centrifuged (500 × *g*) for 10 min. The organic phase (1 ml) was placed in glass tubes and 0.6 ml of Ehrlich's reagent (1:1 ratio of [2.74 ml of 10 *N* H_2SO_4 in 20 ml of 200-proof ethyl alcohol] and [1.2 g *p*-dimethylaminobenzaldehyde in 20 ml 200-proof ethyl alcohol]) was added followed by immediate vortexing. After standing at room temperature for 40 min, samples were read on a Shimadzu ultraviolet–visible (UV-VIS) recording spectrophotometer (Shimadzu Scientific Instruments, Columbia, MD) at 560 nm against a blank. Hydroxyproline content was quantitated from the standard curve and expressed as total hydroxyproline per lung (μg hydroxyproline detected multiplied by 11).

Lung Histopathology

Lung histopathology was performed as previously described (Hubbs et al., 2002). Briefly, mice were weighed and euthanized with an intraperitoneal injection of sodium pentobarbital (>100 mg/kg). The abdominal aorta was transected for exsanguination. The lungs were removed and weighed (lung wet weight). Whole lungs were inflated with 1 ml of 10% neutral buffered formalin. Tissues were trimmed the same day, with sections of the right and left lung lobes and the tracheobronchial lymph node, if found, also trimmed. Tissues were processed overnight and embedded the following day in paraffin. Slides were stained with hematoxylin and eosin (H&E). All slides were interpreted blindly by a board-certified veterinary pathologist. Pathology scores for each section were the sum of the distribution (0 = none, 1 = focal, 2 = locally extensive, 3 = multifocal, 4 = multifocal and coalescent, 5 = diffuse) and severity

scores (0 = none, 1 = minimal, 2 = mild, 3 = moderate, 4 = marked, 5 = diffuse) as previously described by Hubbs et al. (1997). The final pathology score was the mean of the pathology scores from the left and right lung sections of each mouse.

Statistical Analysis

Statistical significance was obtained using a Tukey's test following analysis of variance (ANOVA) with $p \leq 0.05$. In the cases where cells were pooled from multiple mice, the n is indicative of the number of individual experiments and not the number of mice pooled (i.e., 2–3 mice pooled equaled an $n = 1$). For histopathology scoring, a Wilcoxon score (rank sums) nonparametric test was used.

RESULTS

Bronchoalveolar Lavage Alveolar Macrophage Yield

Figure 1 shows the AM yield from WT and iNOS KO mice exposed to silica at 24 h (panel A) and 42 d postexposure (panel B). There was a significant decrease, from the respective control, in number of AMs harvested by bronchoalveolar lavage at 24 h postexposure. AM yield returned to control levels at 42 d postexposure. There was a significant difference between the WT and iNOS KO silica-treated AM yield at 24 h but not 42 d postexposure. Note: No differences were found between the WT and iNOS KO control AM yields at 24 h or 42 d after exposure to saline.

Bronchoalveolar Lavage Polymorphonuclear Leukocyte Yield

Figure 2 represents the PMN yield from WT and iNOS KO mice 24 h (panel A) and 42 d (panel B) postexposure. After exposure to silica, there was a significant increase, from the respective control, in PMNs at 24 h for the WT and iNOS KO. At 42 d postexposure to silica, further increases in PMNs were evident for the WT and iNOS KO mice. Note: No significant difference was found between the WT and iNOS KO PMN counts at 24 h or 42 d from either control or silica-exposed mice.

First Bronchoalveolar Lavage Fluid Lactate Dehydrogenase

First BAL fluid LDH activity, a measure of cytotoxicity, is shown in Figure 3. Panels A and B represent 24 h and 42 d postexposure to silica, respectively. LDH activity was significantly increased from the corresponding WT or iNOS KO control at 24 h postexposure to silica. At 42 d postexposure, silica-induced cytotoxicity in the WT and iNOS KO mice remained significantly elevated from the respective control. The iNOS KO mice, however, exhibited significantly less silica-induced cytotoxicity as compared to WT mice. Note: No significant difference was found between the WT and iNOS KO control levels at 24 h or 42 d.

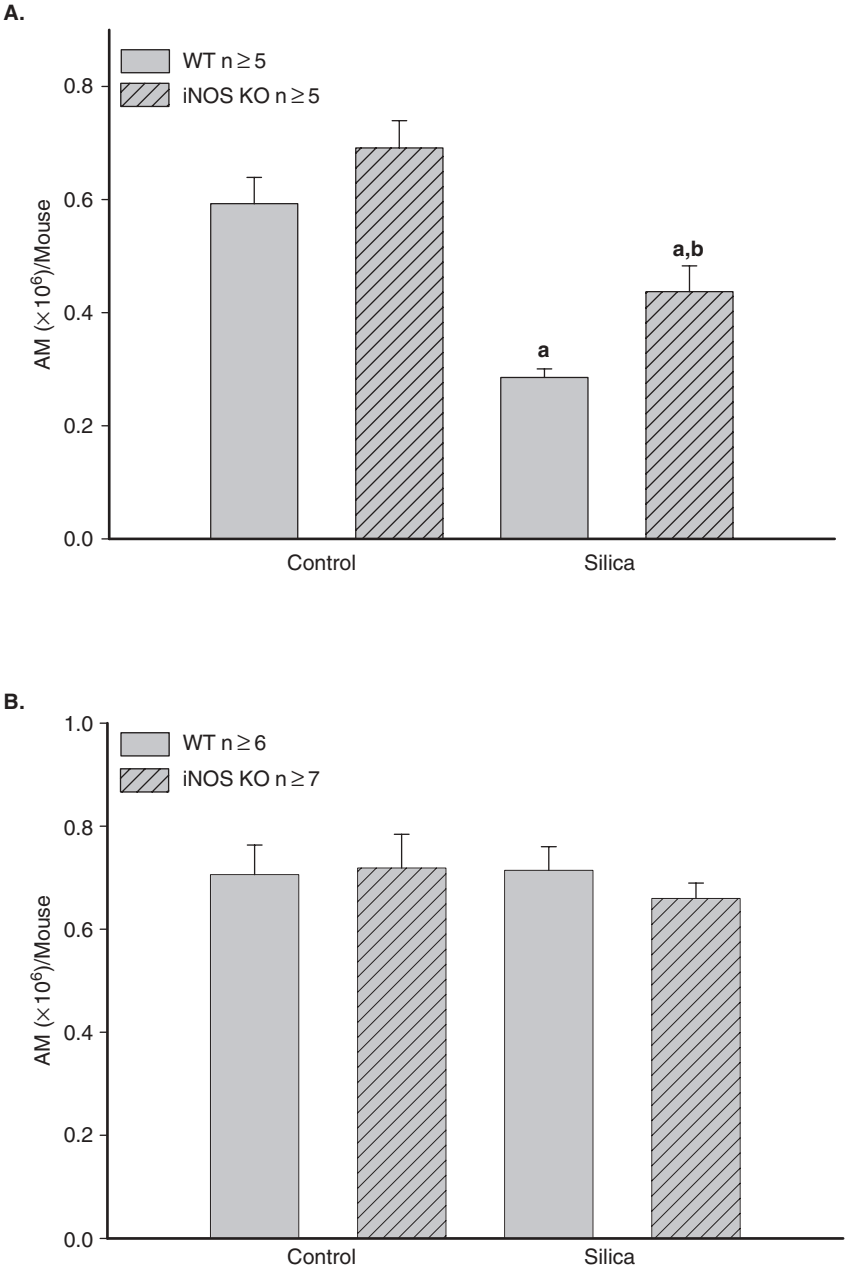

FIGURE 1. Alveolar macrophage yield per mouse at (A) 24 h and (B) 42 d postexposure to silica or saline vehicle. Letter a indicates a significant decrease from the corresponding control alveolar macrophage yield at 24 h; b indicates a significant difference between the WT and iNOS KO groups ($p \leq .05$).

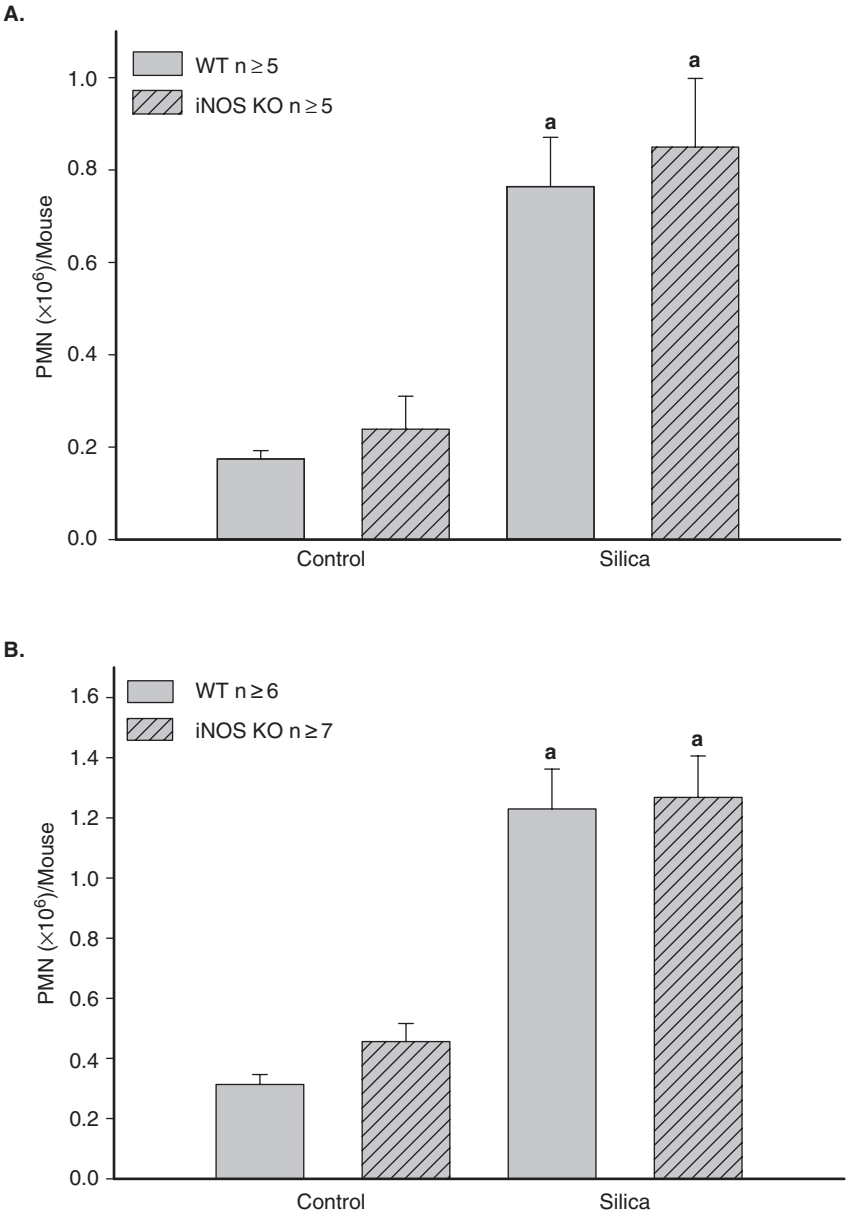

FIGURE 2. Polymorphonuclear leukocyte yield per mouse at (A) 24 h and (B) 42 d postexposure to silica or saline vehicle. Letter a indicates a significant increase from the corresponding control polymorphonuclear leukocyte yield ($p \leq .05$).

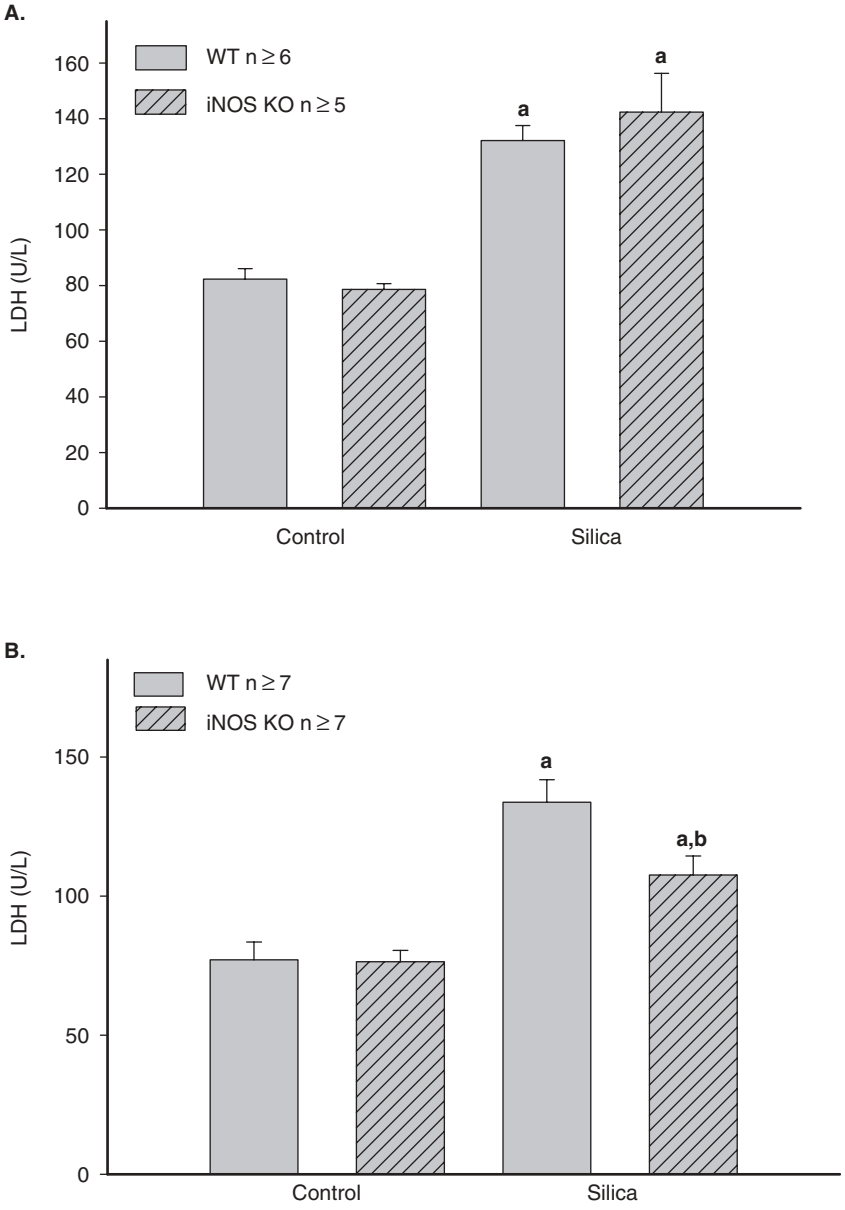

FIGURE 3. First bronchoalveolar lavage fluid lactate dehydrogenase activity at (A) 24 h and (B) 42 d post-exposure to silica or saline vehicle. Letter a indicates a significant increase from the corresponding control lactate dehydrogenase activity; b indicates a significant difference between the iNOS KO and WT treated groups ($p \leq .05$).

First Bronchoalveolar Lavage Fluid Albumin

An indicator of damage to the air-blood barrier is first BAL fluid albumin concentration (Figure 4). Albumin was significantly increased by silica exposure, to the same extent, in both WT and iNOS KO mice at 24 h postexposure (panel A). By 42 d postexposure, silica-induced air–blood barrier damage decreased somewhat in both the WT and iNOS KO (panel B). Although values remained significantly elevated from control, the iNOS KO mice exhibited a marked attenuation of air–blood barrier damage by 42 d postexposure in comparison to the WT. Note: No differences were found between the control states at either 24 h or 42 d. In addition, respective control levels did not differ at either 24 h or 42 d between the WT and iNOS KO mice.

Lung Wet Weight

Figure 5 represents the whole lung wet weight (indicative of pulmonary edema, lipoproteinosis, and/or increased matrix proteins) at 42 d after exposure to silica. Greater pulmonary mass was found in the WT mice as shown by a significant increase from control lung wet weight. In contrast, lung wet weight did not change in response to silica exposure in the iNOS KO mice.

First Bronchoalveolar Lavage Fluid Tumor Necrosis Factor-α

Concentrations of the inflammatory cytokine TNF-α were significantly increased from control levels in the WT and iNOS KO mice at 24 h after silica exposure (Figure 6A). By 42 d after silica exposure (Figure 6B), TNF-α levels had decreased when analyzed as a percent of control (data not shown). However, silica-induced TNF-α levels at 42 d postexposure remained significantly elevated from control in the WT but not in the iNOS KO mice, and TNF-α levels of iNOS KO mice were significantly lower than for WT at this time. Note: Control levels of TNF-α did not differ between the WT and iNOS KO mice at either timepoint.

First Bronchoalveolar Lavage Fluid Macrophage Inflammatory Protein-2

At 24 h postexposure to silica, MIP-2 levels in BAL fluid were significantly increased for both the WT and iNOS KO mice with no significant difference between the WT and iNOS KO mice at this time (Figure 7A). At 42 d postexposure to silica, levels of MIP-2 in the first BAL remained significantly elevated from the respective controls and again did not differ between the WT and iNOS KO (Figure 7B) mice. Note: Control levels of MIP-2 did not differ between the WT and iNOS KO at 24 h or 42 d. From 24 h to 42 d postexposure to silica, levels of MIP-2 did not significantly change in the WT mice, however, levels significantly decreased in the iNOS KO mice.

First Bronchoalveolar Lavage Fluid Total Antioxidant Capacity

The total antioxidant capacity is represented in Figure 8 for the 24-h (panel A) and 42-d (panel B) timepoints. At 24 h and 42 d postexposure to

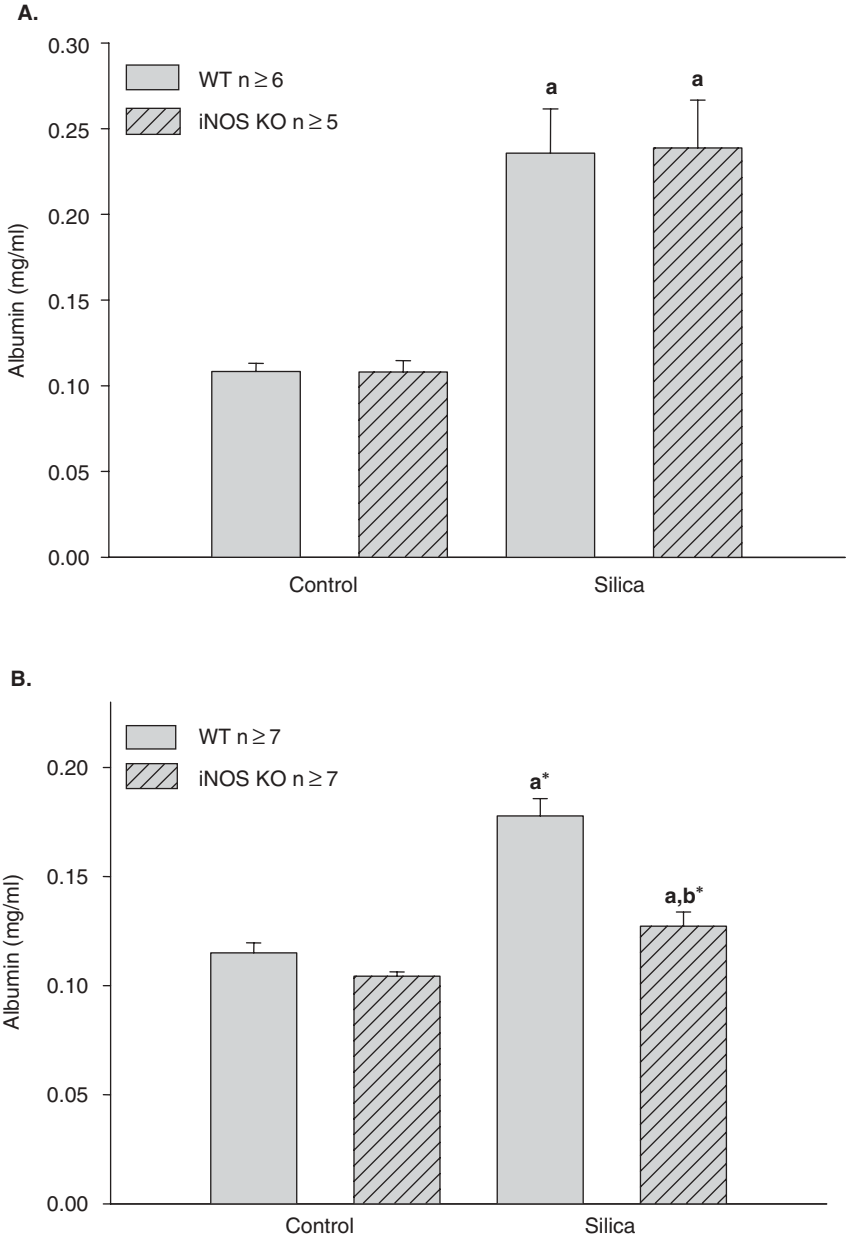

FIGURE 4. First bronchoalveolar lavage fluid albumin at (A) 24 h and (B) 42 d postexposure to silica or saline vehicle. Letter a indicates a significant increase from the corresponding control albumin levels; b indicates a significant difference between the iNOS KO and WT treated groups; asterisk indicates a significant decrease between the 24-h and 42-d corresponding treated groups ($p \leq .05$).

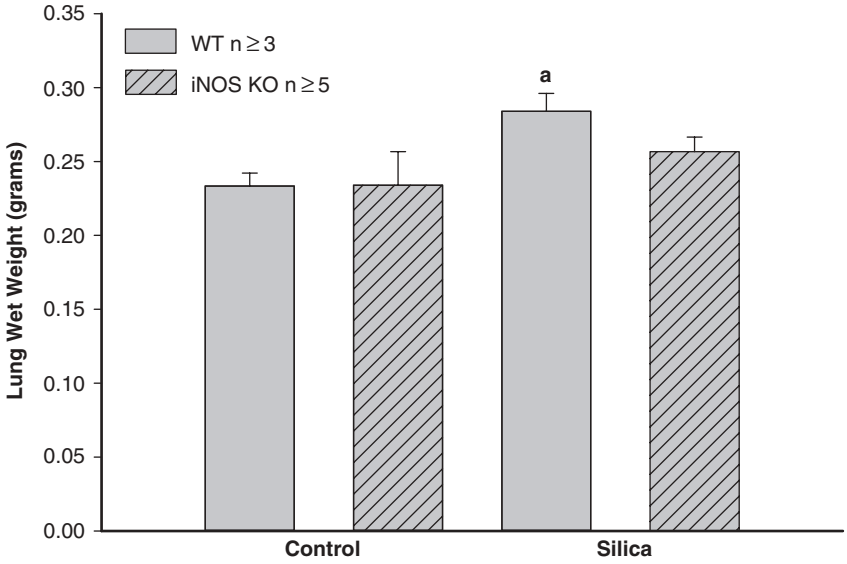

FIGURE 5. Lung wet weight at 42 d postexposure to silica or saline vehicle. Letter a indicates a significant increase from the WT control ($p \leq .05$).

silica, levels of antioxidants were significantly decreased in the WT but were maintained in the iNOS KO mice. Note: Control total antioxidant capacity at 24 h or 42 d did not differ between the WT and iNOS KO mice.

Basal NOx Production by WT Alveolar Macrophages Ex Vivo: Nitrate (NO_3^-) and Nitrite (NO_2^-)

At 42 d postexposure, silica-exposed WT AMs had increased basally produced NOx concentrations, approximately five fold over the control AMs (data not shown). AMs harvested from WT mice 24 h postexposure to silica did not exhibit a change in basal NOx production compared to saline control (data not shown). It was shown previously that phagocytes from iNOS KO mice do not produce NO in response to various stimulants (Zeidler et al., 2003).

Primary Mouse Alveolar Macrophage Zymosan-Stimulated Chemiluminescence

The reactive species production of the iNOS KO AMs, previously exposed to silica in vivo, was significantly less than for the WT upon ex vivo stimulation with zymosan at 24 h and 42 d postexposure (Figure 9). At 24 h postexposure, the WT AMs exhibited approximately a 2.5-fold higher zymosan-stimulated AM-CL compared to the iNOS KO AMs (Figure 9A). At 42 d postexposure, levels of AM-CL decreased in both types of mice but were still significantly elevated from the respective controls (WT AMs exhibited approximately a two fold higher AM-CL compared to iNOS KO AMs) (Figure 9B). Note: Control AM-CL did not differ at either time point between the WT and iNOS KO mice.

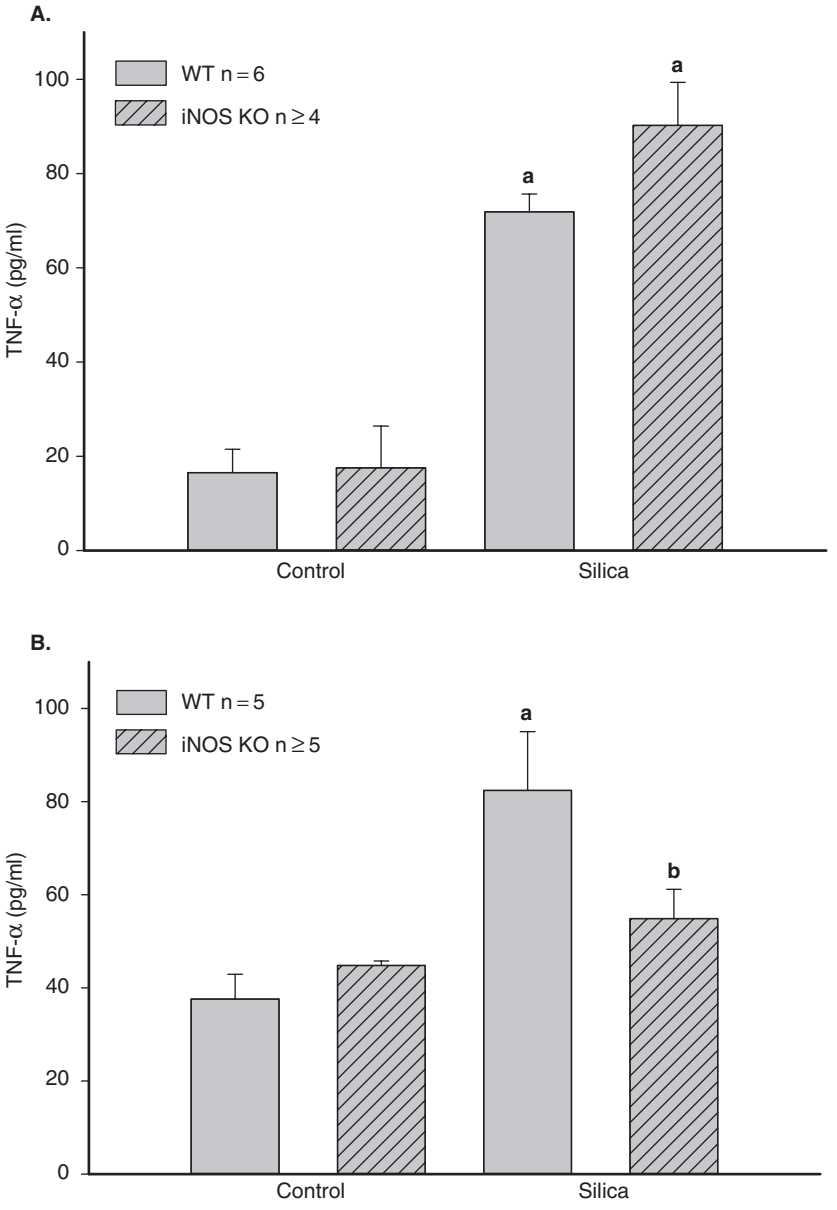

FIGURE 6. First bronchoalveolar lavage fluid TNF-α at (A) 24 h and (B) 42 d postexposure to silica or saline vehicle. Letter a indicates a significant increase from the corresponding control TNF-α levels; b indicates a significant difference between the iNOS KO and WT treated groups ($p \leq .05$).

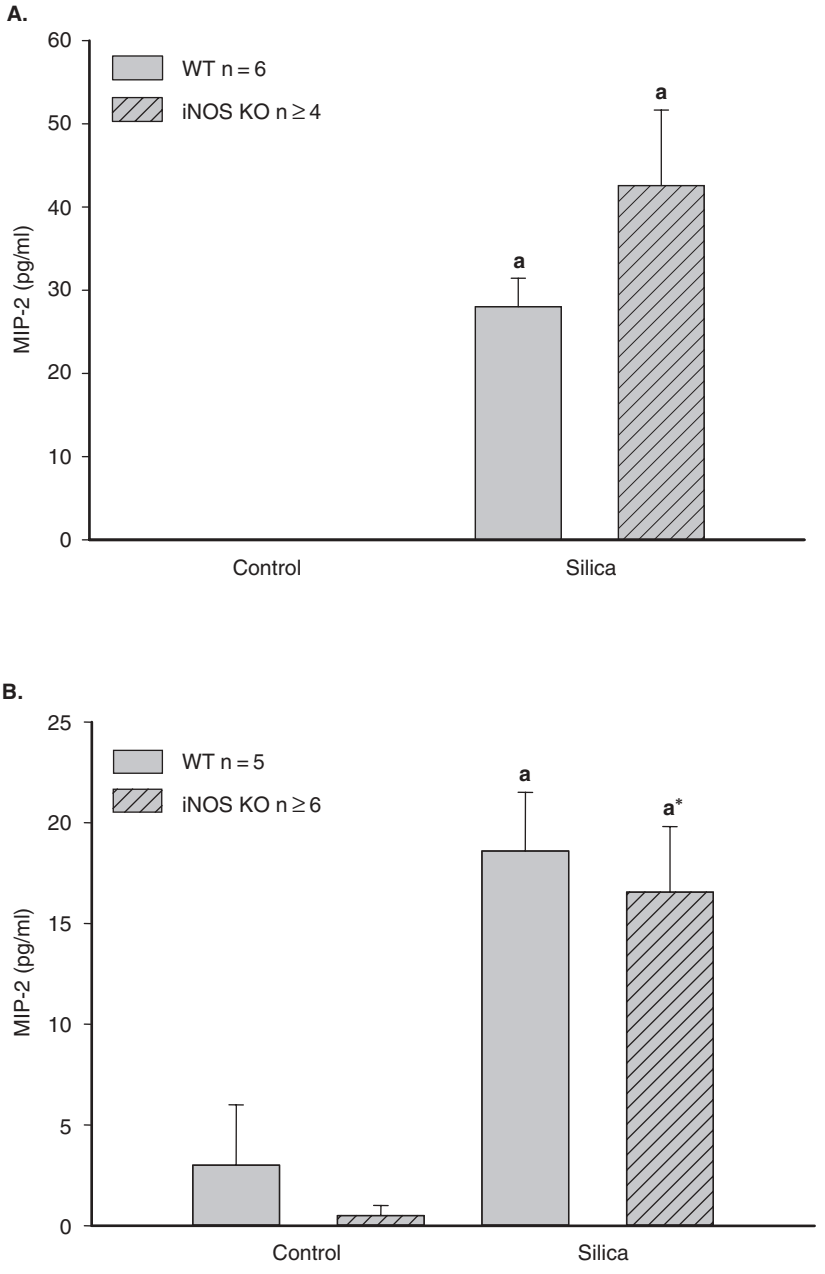

FIGURE 7. First bronchoalveolar lavage fluid MIP-2 at (A) 24 h and (B) 42 d postexposure to silica or saline vehicle. Letter a indicates a significant increase from the corresponding control MIP-2 levels; asterisk indicates a significant decrease at 42 d compared to 24 h postexposure to silica ($p \leq .05$).

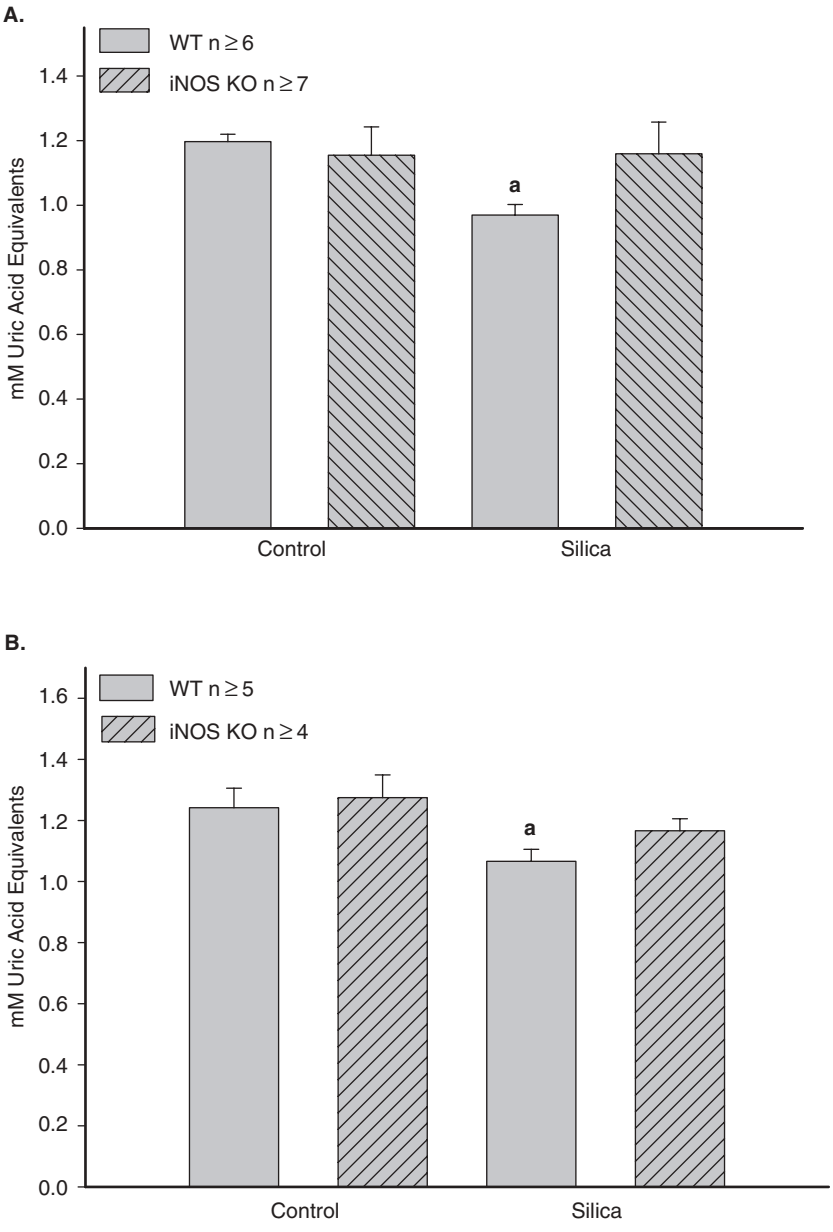

FIGURE 8. First bronchoalveolar lavage fluid total antioxidant capacity at (A) 24 h and (B) 42 d postexposure to silica or saline vehicle. Letter a indicates a significant decrease from the corresponding control total antioxidant capacity ($p \leq .05$).

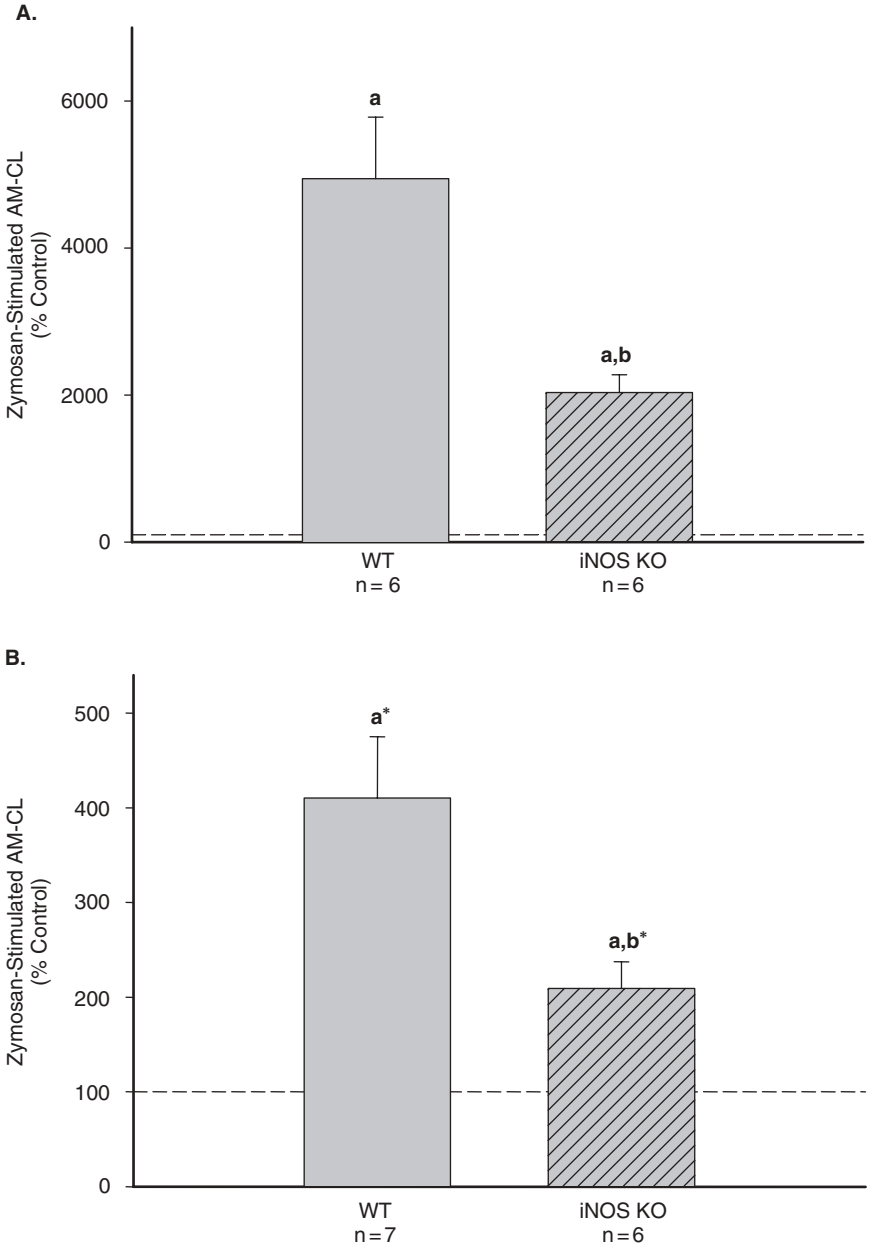

FIGURE 9. Zymosan-stimulated alveolar macrophage chemiluminescence at (A) 24 h and (B) 42 d post-exposure to silica or saline vehicle. Data are presented as percent of control (dashed line represents 100%). Letter a, indicates a significant increase from the corresponding control zymosan-stimulated chemiluminescence; b indicates a significant difference between the iNOS KO and WT treated groups at 24 h or 42 d; asterisk indicates a significant difference between the 24-h and 42-d AM-CL in the corresponding group ($p \leq .05$).

First Bronchoalveolar Lavage Fluid Transforming Growth Factor-β1

At 42 d post silica exposure, TGF-β1 levels in the first BAL fluid were significantly increased from control for both the WT and iNOS KO mice (Figure 10). However, no difference was noted between the WT and iNOS KO mice. Note: Control levels of TGF-β1 did not differ between the WT and iNOS KO mice at 42 d postexposure.

Whole-Lung Hydroxyproline

Lung hydroxyproline content was assessed to determine pulmonary fibrosis at 42 d postexposure to silica in the WT and iNOS KO mice (Figure 11). It was found that the WT mice exhibited significant pulmonary fibrosis compared to control (approximately 26% over control), while the iNOS KO mice did not (approximately 3% over control). The fibrotic response of the WT mice was significantly greater than the iNOS KO mice.

Lung Histopathology

Table 1 represents the histopathology scores for the WT and iNOS KO mice at 42 d postexposure to silica. Representative lung tissue sections, stained with H&E, are shown in Figure 12. Silica exposure increased histological evidence for alveolitis and lipoproteinosis from saline control levels for both WT and iNOS KO mice. Statistically significant differences were found between the WT and iNOS KO mice for the severity and distribution of alveolitis and

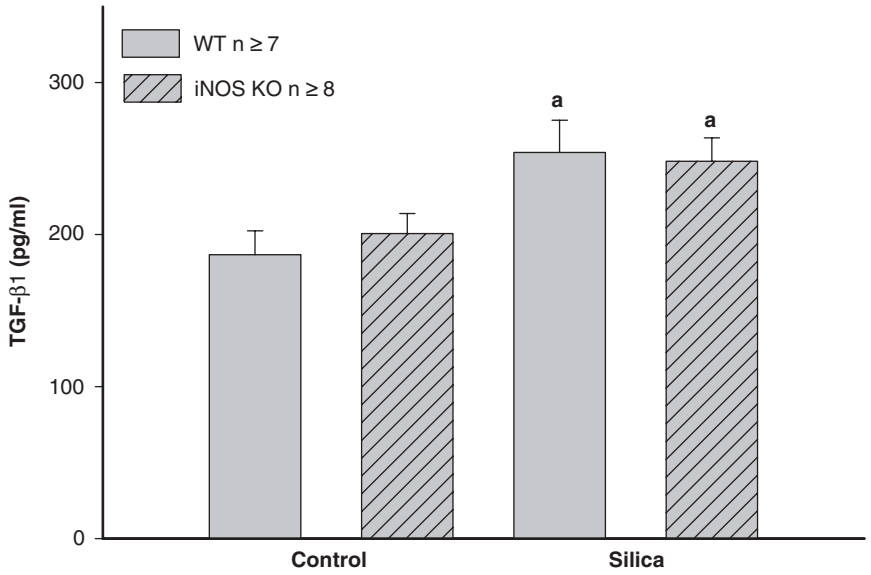

FIGURE 10. First bronchoalveolar lavage fluid TGF-β levels at 42 d postexposure to silica or saline vehicle. Letter a indicates a significant increase from the corresponding control TGF-β levels ($p \leq .05$).

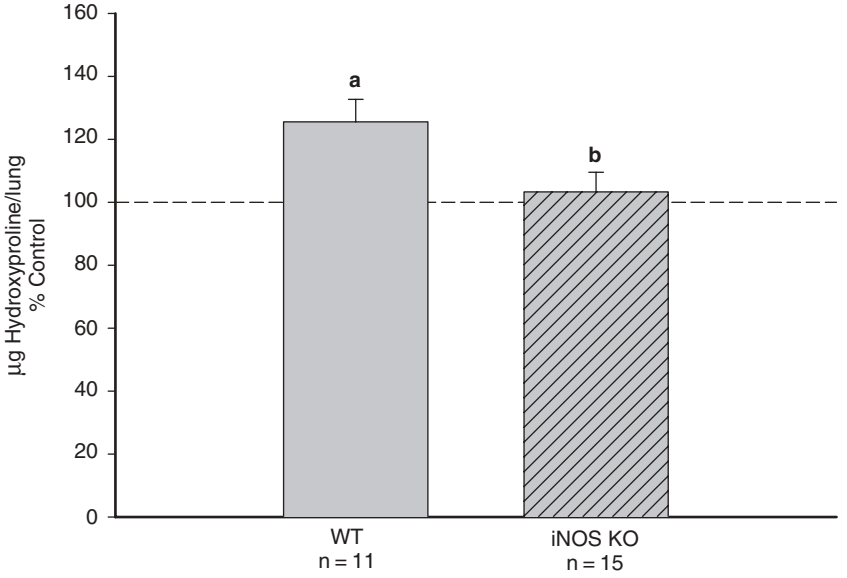

FIGURE 11. Lung hydroxyproline content at 42 d postexposure to silica or saline vehicle. Data are presented as percent of control (dashed line represents 100%). Letter a indicates a significant increase in fibrosis from the corresponding control; b indicates a significant difference between the iNOS KO and WT treated groups ($p \leq .05$).

TABLE 1. Histopathology Scores at 42 d Post Silica Exposure

	Control	WT	iNOS KO
Alveolitis	0	4.8 ± 0.3^{a}	$2.3 \pm 0^{a,b}$
Lipoproteinosis	0	4.7 ± 0.46^{a}	$1.9 \pm 0^{a,b}$

Note. Values represent the sum of the lesion severity and distribution scores and are means ± SE ($n \geq 3$). Histologic scores for both WT and iNOS KO control mice were 0 for both alveolitis and lipoproteinosis.

[a] Significant difference from the corresponding control.

[b] Significant difference between the WT and iNOS KO mice ($p \leq 0.05$).

lipoproteinosis; that is, silica exposure resulted in approximately 50% less alveolitis and lipoproteinosis in the iNOS KO mice compared to the WT mice after 42 d.

DISCUSSION

The objective of this study focused on NO derived from iNOS and its role in the acute and subchronic response to silica in iNOS KO and WT (C57Bl/6J—background strain) mice. It was observed that iNOS KO mice exhibited lower AM-CL and a maintained total antioxidant capacity compared to WT mice at 24 h postexposure to silica. At 42 d post silica exposure, iNOS KO mice exhibited less pulmonary damage, oxidative stress (lower AM-CL and

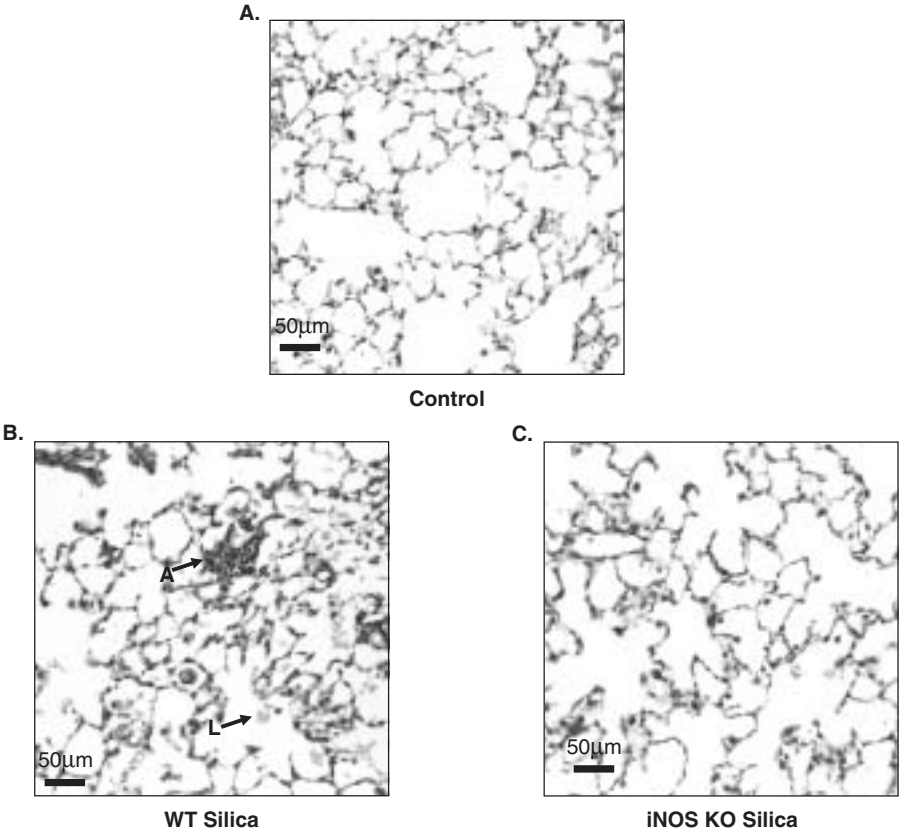

FIGURE 12. Photomicrograph of (A) control lung, (B) WT silica-exposed lung, and (C) iNOS KO silica-exposed lung at 42 d postexposure. Alveolitis (A) and lipoproteinosis (L) are evident in the silica-exposed lungs as indicated. Neither alveolitis nor lipoproteinosis was seen in any control lungs from either WT or iNOS KO mice.

maintained antioxidant capacity), and TNF-α production than WT mice. In addition, markers of lung fibrosis and histopathological scores for alveolitis and lipoproteinosis revealed an attenuated subchronic response to silica in the iNOS KO mice, suggesting iNOS-derived NO assumes a deleterious role in this experimental model.

Following acute exposure to silica, AM yield in the iNOS KO mice differed significantly from the WT mice. It has been reported that lavageable AMs may decrease following acute exposure to certain occupational dusts due to AM activation and increased adherence to the alveolar wall (Castranova et al., 1987b). Therefore, the stronger adherence to the alveolus makes recovery by BAL difficult, resulting in a lower yield, implying a higher AM activation status (Castranova et al., 1987b). The present study observed higher lavageable AMs in the iNOS KO mice, compared to the WT mice, 24 h after silica exposure. By

42 d post silica exposure, AMs harvested from the WT and iNOS KO mice returned to control levels and these yields (control or treated) were not different between the two types of mice. Histologically, increased rather than decreased numbers of phagocytic cells (including AMs) were evident in the alveolar space of both the WT and iNOS KO lungs 42 d postexposure versus control lungs. Thus, BAL recovery only serves as an approximate indicator of the in vivo situation and should not be considered solely.

As mentioned earlier, the AM yield data implied a lower silica-induced activation status of the iNOS KO AMs. This was further supported by a decreased zymosan stimulated AM-CL for iNOS KO mice compared to the WT AMs at both 24 h and 42 d postexposure to silica. Furthermore, total antioxidant capacity in the first BAL, a nonspecific measure of antioxidants from all pulmonary cell types, was maintained after silica exposure in the iNOS KO but significantly decreased from control in silica-exposed WT mice at both time points. Considered together, lower AM-CL and maintenance of total antioxidant capacity indicate a lower silica-induced lung oxidant burden in the iNOS KO mice.

The data show that the absence of iNOS-derived NO did not affect the levels of the TNF-α and MIP-2 in the first BAL fluid following acute silica exposure; that is, both the WT and iNOS KO mice had equally elevated levels of these inflammatory mediators versus the respective control. At 42 d postexposure to silica, however, TNF-α remained elevated versus control in the WT but not in the iNOS KO mice. It has been reported that silica-induced reactive species, including NO, may regulate TNF-α gene expression, possibly through the transcription factor NF-κB (Baeuerle, 1991; DeForge et al., 1993; Gossart et al., 1996; Rojanasakul et al., 1997; Savici et al., 1994). TNF-α is an important proinflammatory cytokine that has been implicated in the initiation and progression of pulmonary fibrosis (Piguet & Vesin, 1994). The present study supports the notion that silica-induced oxidant stress may influence NF-κB activation and subsequent TNF-α production, and that NO plays a role in this oxidant stress.

PMNs were increased equally by exposure to silica in both the WT and iNOS KO mice after 24 h. Silica-induced PMNs further increased by 42 d. This correlates with the equally elevated MIP-2 levels in WT and iNOS KO mice exposed to silica. Evidence does exist that NO attenuates leukocyte adhesion and recruitment into the lung in certain models of lung inflammation (Gaston et al., 1994; Hickey & Kubes, 1997; Lin et al., 2001; Sato et al., 1999). However, no marked difference in PMN infiltration in iNOS KO mice was observed in this experimental model.

Markers of lung injury and blood–air barrier damage, measured as LDH activity and albumin concentration, respectively, were comparably increased in the WT and iNOS KO mice 24 h after silica exposure. By 42 d, these markers were attenuated in the iNOS KO mice versus the WT but remained elevated above the respective control. In addition, lung wet weight, at 42 d postexposure to silica, was elevated in the WT but not in the iNOS KO. These

data suggest that the absence of NO derived from iNOS appears to exert a beneficial role, in terms of lung injury, which is more evident in the subchronic model than the acute model of silica exposure.

The subchronic inflammatory phase was also evaluated via histopathology (Figure 12 and Table 1). The lung sections and pathology scores noted significant attenuation of alveolitis and lipoproteinosis, that is, inflammatory cell infiltration into the alveoli and increased production of phospholipids and surfactant proteins by alveolar Type II epithelial cells, respectively, in the iNOS KO versus the WT mice 42 d after silica exposure. The BAL data showed no differences in cell yields between the WT and iNOS KO mice at 42 d postexposure. As mentioned, BAL recovery of activated phagocytes is often difficult; therefore, histopathological analysis may be a more adequate determinant of the extent of the alveolitis. The histopathology data complemented the other parameters measured that revealed less injury and damage in the iNOS KO mice in the subchronic phase of the response to silica.

Whole-lung hydroxyproline analysis for pulmonary fibrosis showed a statistically significant difference existed between the WT and iNOS KO mice, with the silica-induced fibrotic response being significantly greater than control only in WT mice. This decreased fibrotic response in iNOS KO mice in response to silica exposure correlates with lower inflammation and damage and less AM activation in iNOS KO mice 42 d postexposure.

Both animal and human data support a detrimental role for NO in silica-induced lung injury and disease as mentioned previously (Blackford et al., 1994; Kang et al., 2000; Porter et al., 2002; Castranova et al., 1998). The present data agree with those reported by Porter et al. (2002), which indicated a temporal and anatomical relationship between iNOS induction and pulmonary response to silica and suggested that iNOS-derived NO is involved in the progression of silica-induced lung disease. A mouse silica inhalation study (250 mg/m^3, 5 h/d for 10 d) by Srivastava et al. (2002) also correlates with the present findings. However, Srivastava and colleagues noted that at 1, 6, and 12 wk after exposure, silica did not induce significant pulmonary inflammation in the iNOS KO mice. These data do not agree with the present report, where at 24 h marked lung inflammation was observed that was comparable between the WT and iNOS KO mice, and this inflammation remained elevated above control, but less so in iNOS KO mice, at 42 d postexposure. It is likely this may be due to differences such as, exposure dose and method (aspiration [40 mg/kg] vs. inhalation [250 mg/m^3]), analysis (BAL parameters and histopathology vs. histopathology alone), and time points (24 h and 42 d vs. 1, 6, and 12 wk) between the present study and Srivastava et al. (2002). In general, however, both studies conclude that absence of iNOS-derived NO reduces the pulmonary response to silica.

In contrast to the present data, it has been reported that the absence of NO from iNOS enhances pulmonary inflammation in response to various stimuli. For example, asbestos instillation in iNOS KO mice resulted in attenuated oxidant-promoted lung tissue damage, but inflammatory parameters, such as

TNF-α production and neutrophil influx, were increased in the iNOS KO versus the WT (Dorger et al., 2002). NO, in acute lung injury induced by ozone, has been associated with both enhanced damage and protection in studies using iNOS KO mice (Fakhrzadeh et al., 2002; Kenyon et al., 2002). Furthermore, hyperoxia-induced acute lung injury is increased in the absence of iNOS (Kobayashi et al., 2001). Susceptibility to certain microbial pathogens has also been reported in iNOS KO mice, including respiratory challenge with *Bordetella pertussis* (Canthaboo et al., 2002).

In summary, the role of NO in the acute response to silica centered on the oxidant status of the lung. Due to the absence of iNOS, the formation $OONO^-$ is limited, thus possibly accounting for the majority of the decreased lung oxidant burden. The silica-induced lung response in the longer term was significantly less in the iNOS KO mice, but some evidence of pulmonary damage and inflammation was still noted in these animals. This suggests that NO derived from iNOS contributes to the pathogenesis of silica-induced lung disease in the mouse model but does not account for all of the lung pathology. Perhaps contributions from other inflammatory mediators or reactive species produced by cells or silica particles directly account for the injury and damage still observed in the iNOS KO mice. TNF-α has been proposed as an important initiator of the inflammatory and fibrotic response of the lung to silica exposure (Driscoll & Guthrie, 1997). Indeed, treatment of mice with TNF-α antibody has been reported to be protective against silica-induced pulmonary fibrosis (Piguet et al., 1990). Recently, Srivastava et al. (2002) suggested that interleukin-1 beta (IL-1β) was a key mediator of silica-induced pulmonary response. They reported that silica-induced iNOS expression, apoptosis, and histopathological evidence of inflammatory lesions were significantly lower in IL-1β knockout mice compared to wild-type mice. However, neither TNF-α or IL-1β appears to the sole driver of pulmonary responses to silica, since Castranova et al. (2002) noted that most markers of silica-induced pulmonary damage, inflammation, and fibrosis appear to precede a marked increase in TNF-α or IL-1β levels in the bronchoalveolar lavage fluid in a rat inhalation model. It is likely that the pulmonary response to silica is complex and is affected by interplay of multiple oxidants, chemokines, and cytokines (Castranova, 2000).

REFERENCES

Allen, R. C. 1977. Evaluation of serum opsonic capacity by quantitating the initial chemiluminescent response from phagocytizing polymorphonuclear leukocytes. *Infect. Immun.* 15:828–833.

Baeuerle, P. A. 1991. The inducible transcription activator NF-kappa B: Regulation by distinct protein subunits. *Biochim. Biophys. Acta* 1072:63–80.

Blackford, J. A., Jr., Antonini, J. M., Castranova, V., and Dey, R. D. 1994. Intratracheal instillation of silica up-regulates inducible nitric oxide synthase gene expression and increases nitric oxide production in alveolar macrophages and neutrophils. *Am. J. Respir. Cell Mol. Biol.* 11:426–431.

Blackford, J. A., Jr., Jones, W., Dey, R. D., and Castranova, V. 1997. Comparison of inducible nitric oxide synthase gene expression and lung inflammation following intratracheal instillation of silica, coal, carbonyl iron, or titanium dioxide in rats. *J. Toxicol. Environ. Health* 51:203–218.

Canthaboo, C., Xing, D., Wei, X. Q., and Corbel, M. J. 2002. Investigation of role of nitric oxide in protection from *Bordetella pertussis* respiratory challenge. *Infect. Immun*. 70:679–684.

Castranova, V. 2000. From coal mine dust to quartz: Mechanisms of pulmonary pathogenicity. *Inhal. Toxicol*. 12(suppl. 3):7–14.

Castranova, V., Lee, P., Ma, J. Y. C., Weber, K. C., Pailes, W. H., and Miles, P. R. 1987a. Chemiluminescence from macrophages and monocytes In *Cellular chemiluminescence*, eds. K. Van Dyke and V. Castranova, pp. 4–19. Boca Raton, FL: CRC.

Castranova, V., Robinson, V. A., Tucker, J. H., Schwegler, D., Rose, D. A., Delong, D. S., and Frazer, D. G. 1987b. Time course of pulmonary response to inhalation of cotton dust. In *Proceedings of the 14th Cotton Dust Research Conference*, eds. R. R., Jacobs, P. J., Wakelyn, and L. N. Domelsmith pp. 79–83. Memphis, TN: National Cotton Council.

Castranova, V., Jones, T. A., Barger, M. W., Afshari, A., and Frazer, D. G. 1990. Pulmonary responses of guinea pigs to consecutive exposures to cotton dust. In *Proceedings of the 14th Cotton Dust Research Conference*, eds. R. R. Jacobs, P. J. Wakelyn, and L. N. Domelsmith, pp. 131–135. Memphis, TN: National Cotton Council.

Castranova, V., Huffman, L. J., Judy, D. J., Bylander, J. E., Lapp, L. N., Weber, S. L., Blackford, J. A., and Dey, R. D. 1998. Enhancement of nitric oxide production by pulmonary cells following silica exposure. *Environ. Health Perspect*. 106(suppl. 5):1165–1169.

Castranova, V., Porter, D., Millecchia, L., Ma, J. Y. C., Hubbs, A. F., and Teass, A. 2002. Effect of inhaled crystalline silica in a rat model: Time course of pulmonary reactions. *Mol. Cell. Biochem*. 234/235:177–184.

Chen, F., Kuhn, D. C., Sun, S. C., Gaydos, L. J., and Demers, L. M. 1995. Dependence and reversal of nitric oxide production on NF-kappa B in silica and lipopolysaccharide-induced macrophages. *Biochem. Biophys. Res. Commun*. 214:839–846.

Daniel, L. N., Mao, Y., and Saffiotti, U. 1993. Oxidative DNA damage by crystalline silica. *Free Radical Biol. Med*. 14:463–472.

DeForge, L. E., Preston, A. M., Takeuchi, E., Kenney, J., Boxer, L. A., and Remick, D. G. 1993. Regulation of interleukin 8 gene expression by oxidant stress. *J. Biol. Chem*. 268:25568–25576.

Dorger, M., Allmeling, A. M., Kiefmann, R., Schropp, A., and Krombach, F. 2002. Dual role of inducible nitric oxide synthase in acute asbestos-induced lung injury. *Free Radical Biol. Med*. 33:491–501.

Driscoll, K. E., and Guthrie, G. D. 1997. Crystalline silica and silicosis. In *Comprehensive Toxicology, Vol. 8 Toxicology of the Respiratory System*, ed. R. A. Roth, pp. 373–391. New York, NY: Elsevier Sciences Inc.

Fakhrzadeh, L., Laskin, J. D., and Laskin, D. L. 2002. Deficiency in inducible nitric oxide synthase protects mice from ozone-induced lung inflammation and tissue injury. *Am. J. Respir. Cell Mol. Biol*. 26:413–419.

Gaston, B., Drazen, J. M., Loscalzo, J., and Stamler, J. S. 1994. The biology of nitrogen oxides in the airways. *Am. J. Respir. Crit. Care Med*. 149:538–551.

Gossart, S., Cambon, C., Orfila, C., Seguelas, M. H., Lepert, J. C., Rami, J., Carre, P., and Pipy, B. 1996. Reactive oxygen intermediates as regulators of TNF-alpha production in rat lung inflammation induced by silica. *J. Immunol*. 156:1540–1548.

Haddad, I. Y., Zhu, S., Crow, J., Barefield, E., Gadilhe, T., and Matalon, S. 1996a. Inhibition of alveolar type II cell ATP and surfactant synthesis by nitric oxide. *Am. J. Physiol*. 270:L898–L906.

Haddad, I. Y., Zhu, S., Ischiropoulos, H., and Matalon, S. 1996b. Nitration of surfactant protein A results in decreased ability to aggregate lipids. *Am. J. Physiol*. 270:L281–L288.

Hickey, M. J., and Kubes, P. 1997. Role of nitric oxide in regulation of leucocyte-endothelial cell interactions. *Exp. Physiol*. 82:339–348.

Hill, H. R., Hogan, N. A., Bale, J. F., and Hemming, V. G. 1977. Evaluation of nonspecific (alternative pathway) opsonic activity by neutrophil chemiluminescence. *Int. Arch. Allergy Appl. Immunol*. 53:490–497.

Hogg, N., and Kalyanaraman, B. 1999. Nitric oxide and lipid peroxidation. *Biochim. Biophys. Acta* 1411:378–384.

Hubbs, A. F., Castranova, V., Ma, J. Y., Frazer, D. G., Siegel, P. D., Ducatman, B. S., Grote, A., Schwegler-Berry, D., Robinson, V. A., Van Dyke, C., Barger, M., Xiang, J., Parker, J. 1997. Acute lung injury induced by a commercial leather conditioner. *Toxicol. Appl. Pharmacol*. 143:37–46.

Hubbs, A. F., Battelli, L. A., Goldsmith, W. T., Porter, D. W., Frazer, D., Friend, S., Schwegler-Berry, D., Mercer, R. R., Reynolds, J. S., Grote, A., Castranova, V., Kullman, G., Fedan, J. S., Dowdy, J., Jones, W. G.

2002. Necrosis of nasal and airway epithelium in rats inhaling vapors of artificial butter flavoring. *Toxicol. Appl. Pharmacol.* 185:128–135.

Kang, J. L., Lee, K., Castranova, V. 2000. Nitric oxide up-regulates DNA-binding activity of nuclear factor-kappa B in macrophages stimulated with silica and inflammatory stimulants. *Mol. Cell. Biochem.* 215:1–9.

Kenyon, N. J., van der Vliet, A., Schock, B. C., Okamoto, T., McGrew, G. M., and Last, J. A. 2002. Susceptibility to ozone-induced acute lung injury in iNOS-deficient mice. *Am. J. Physiol. Lung Cell Mol. Physiol.* 282:L540–L545.

Kivirikko, K. I., Laitinen, O., and Prockop, D. J. 1967. Modifications of a specific assay for hydroxyproline in urine. *Anal. Biochem.* 19:249–255.

Kobayashi, H., Hataishi, R., Mitsufuji, H., Tanaka, M., Jacobson, M., Tomita, T., Zapol, W. M., and Jones, R. C. 2001. Antiinflammatory properties of inducible nitric oxide synthase in acute hyperoxic lung injury. *Am. J. Respir. Cell Mol Biol.* 24:390–397.

Lin, H. C., Wang, C. H., Yu, C. T., Hwang, K. S., and Kuo, H. P. 2001. Endogenous nitric oxide inhibits neutrophil adherence to lung epithelial cells to modulate interleukin-8 release. *Life Sci.* 69:1333–1344.

Ma, J. Y., Barger, M. W., Hubbs, A. F., Castranova, V., Weber, S. L., and Ma, J. K. 1999. Use of tetrandrine to differentiate between mechanisms involved in silica versus bleomycin-induced fibrosis. *J. Toxicol. Environ. Health A* 57:247–266.

Mikawa, K., Nishina, K., Tamada, M., Takao, Y., Maekawa, N., and Obara, H. 1998. Aminoguanidine attenuates endotoxin-induced acute lung injury in rabbits. *Crit. Care Med.* 26:905–911.

Mossman, B. T., and Churg, A. 1998. Mechanisms in the pathogenesis of asbestosis and silicosis. *Am. J. Respir. Crit. Care Med.* 157:1666–1680.

Piguet, P. F., and Vesin, C. 1994. Treatment by human recombinant soluble TNF receptor of pulmonary fibrosis induced by bleomycin or silica in mice. *Eur. Respir. J.* 7:515–518.

Piguet, P. F., Collart, M. A., Grau, G. E., Sappino, A-P., and Vassalli, P. 1990. Requirement for tumour necrosis factor for development of silica-induced pulmonary fibrosis. *Nature* 344:245–247.

Porter, D. W., Millecchia, L., Robinson, V. A., Hubbs, A., Willard, P., Pack, D., Ramsey, D., McLaurin, J., Khan, A., Landsittel, D., Teass, A., and Castranova, V. 2002. Enhanced nitric oxide and reactive oxygen species production and damage after inhalation of silica. *Am. J. Physiol. Lung Cell Mol. Physiol.* 283:L485–L493.

Rao, K. M. K. 2000. Molecular mechanisms regulating iNOS expression in various cell types. *J. Toxicol. Environ. Health B,* 3:27–58.

Rao, G. V. S., Tinkle, S., Weissman, D. N., Antonini, J. M., Kashon, M. L., Salmen, R., Battelli, L. A., Willard, P. A., Hoover, M. D., and Hubbs, A. F. 2003. Efficacy of a technique for exposing the mouse lung to particles aspirated from the pharynx. *J. Toxicol. Environ. Health A* 66:1441–1452.

Rojanasakul, Y., Weissman, D. N., Shi, X., Castranova, V., Ma, J. K., and Liang, W. 1997. Antisense inhibition of silica-induced tumor necrosis factor in alveolar macrophages. *J. Biol. Chem.* 272:3910–3914.

Sato, Y., Walley, K. R., Klut, M. E., English, D., D'Yachkova, Y., Hogg, J. C., and van Eeden, S. F. 1999. Nitric oxide reduces the sequestration of polymorphonuclear leukocytes in lung by changing deformability and CD18 expression. *Am. J. Respir. Crit. Care Med.* 159:1469–1476.

Savici, D., He, B., Geist, L. J., Monick, M. M., and Hunninghake, G. W. 1994. Silica increases tumor necrosis factor (TNF) production, in part, by upregulating the TNF promoter. *Exp. Lung Res.* 20:613–625.

Shi, X., Castranova, V., Halliwell, B., and Vallyathan, V. 1998. Reactive oxygen species and silica-induced carcinogenesis. *J. Toxicol. Environ. Health B* 1:181–197.

Shukla, A., Timblin, C. R., Hubbard, A. K., Bravman, J., and Mossman, B. T. 2001. Silica-induced activation of c-Jun-NH2-terminal amino kinases, protracted expression of the activator protein-1 proto-oncogene, fra-1, and S-phase alterations are mediated via oxidative stress. *Cancer Res.* 61:1791–1795.

Srivastava, K. D., Rom, W. N., Jagirdar, J., Yie, T. A., Gordon, T., and Tchou-Wong, K. M. 2002. Crucial role of interleukin-1beta and nitric oxide synthase in silica-induced inflammation and apoptosis in mice. *Am. J. Respir. Crit. Care Med.* 165:527–533.

Vallyathan, V., Shi, X., and Castranova, V. 1998. Reactive oxygen species: Their relation to pneumoconiosis and carcinogenesis. *Environ. Health Perspect.* 106(suppl. 5):1151–1155.

van der Vliet, A., Eiserich, J. P., Halliwell, B., and Cross, C. E. 1997. Formation of reactive nitrogen species during peroxidase-catalyzed oxidation of nitrite. A potential additional mechanism of nitric oxide-dependent toxicity. *J. Biol. Chem.* 272:7617–7625.

Zeidler, P. C., and Castranova, V. 2004. Role of nitric oxide in pathologic responses of the lung to exposure to environmental/occupational agents. *Redox Rep*. 9:7–18.

Zeidler, P., Roberts, J., Castranova, V., Chen, F., Butterworth, L., Andrew, M., Robinson, V., and Porter, D. 2003. Response of alveolar macrophages from inducible nitric oxide synthase knockout or wild-type mice to an in vitro lipopolysaccharide or silica exposure. *J. Toxicol. Environ. Health A* 66:995–1013.